北海道大学工学部研究報告
第162号（平成4年）

Bulletin of the Faculty of Engineering
Hokkaido University, No. 162 (1992)

TEM OBSERVATION OF MAGNETITE REDUCTION WITH IMPLANTED HYDROGEN

K. ISHII*, M. KATSUMI**, Y. TAMURA***,
Y. KASHIWAYA*, and S. SATOH*

(Received September 18, 1992)

Abstract

In order to make clear the crystallographic mechanism of H_2 reduction of iron oxide, hydrogen ion was implanted into the magnetite and microstructural changes were investigated by a transmission electron microscope (TEM). Magnetite sample was prepared by oxidizing thin foils of pure iron with CO_2 gas at 1300°C. The samples for TEM observation were finally thinned by Ar ion milling. Hydrogen implantation was conducted at room temperature after Ar ion thinning. The energy of implantation was 50 KeV and the doses were 1 and 2×10^{17} ion-H_2/cm^2. In the spot where the defect cluster introduced by Ar thinning was concentrated, wustite phase was formed in the magnetite matrix as soon as hydrogen was implanted. Wustite was also formed by cooperation of hydrogen implanted and electron irradiation during TEM observation.

Key words: Magnetite, ion implantation, crystallographic mechanism, hydrogen reduction

1. Introduction

The reduction mechanism of iron oxides with reactive gas has been studied over a century. These studies were mainly carried out on a macroscopic scale using pellet or sintered ore. Though the results were frequently discussed in view of kinetics, nucleation, and morphology of precipitated phases[1-3], a few of them were also treated from a microscopic point of view. Recently, some reports have been appeared on a use of electron microscope as a probe of studying the microstructural change during oxide reduction[4-6]. However, most of them are ex-situ investigations and the in-situ studies are few. Rau and co-workers pursued direct observation by means of environmental cell in which iron oxide was reduced with H_2 and H_2-Ar mixture[7].

The present investigation is aimed to probe the mechanism of reduction at an atomic scale. Experiments were conducted by using ion implantation technique as a new method of reductant supply to iron oxides. Ion implantation is one of the doping techniques which is

* Department of Metallurgical Engineering, Faculty of Engineering, Hokkaido University
** Formerly department of Metallurgical Engineering, Faculty of Engineering, Hokkaido University
*** Graduate student. the present Mitsubishi Electric Company Ltd

noticed as surface modification method of semiconductor materials and fine ceramics[8)-11)]. In this method, ionized elements in vacuum are accelerated in the electric field and irradiated to solid substrate. Apply ion implantation technique to the reduction experiment, specimens exposed to no cooling and no oxidation conditions as if iron oxide were reduced at room temperature. The microstructural changes were observed by transmission electron microscope (TEM), and the formation mechanism of wustite from magnetite was determined by crystallographic analysis using selected area diffraction (SAD).

2. Experimental apparatus and procedure

Iron oxide specimens were prepared from the thin foils of pure iron (99.99 %). In order to determine the orientation of sample crystals with SAD method, the samples must be single crystals larger than 3mm in diameter. Therefore the pure iron plates were annealed after rolling reduction to cause grain growth before oxidation. At first electrolytic iron plates were cut with the microcutter and rolled to sheets of 0.3mm in thickness at room temperature. After degreasing in acetone, the surface layers of the sheets were removed by hydrochloric acid of 100°C. The sheets were annealed in an electric furnace at 1300°C for 24 hours in Ar, which was dried through silica gel and penta-phosphorus oxide to avoid surface oxidation. After annealing, the atmosphere of Ar was changed to CO_2 at the same temperature and specimens were oxidized and thined by mechanical polishing (16μm SiC powder followed by 1μm alumina powder) to a thickness of approximately 30 μm. Since the specimen was very brittle, stainless ring, which was outer 3mm and inner 1.5mm in diameter, was bonded by epoxy resin to reinforce it. Final thinning for TEM observation was carried out for 25-50 hours by means of an Ar ion milling apparatus, of which anodic voltage was 6kV and ionic current was 0.6mA. Into the specimens which were prepared as mentioned above, hydrogen was implanted at room temperature with ion implanter of which the maximum energy was 300keV. Implantation energy was 50 KeV, ionic current density was 2 μA/cm^2 and the doses were 1 and 2×10^{17} ions/cm^2. It took about 52 minutes to implant 2×10^{17} ions/cm^2. Though the temperature of specimen increased by beam radiation, it allowed to be ignored. If all implanted hydrogen reacts with magnetite as follows,

$$Fe_3O_4+2H=3FeO+H_2O \qquad (1)$$

about 27 % of magnetite oxygen in irradiated area is removed in thickness of 3000 Å.

The change of structure before and after ion implantation was observed with a 200kV TEM. The crystallographic relationship between magnetite and wustite formed was determined by SAD. Then the ion-implanted specimens were irradiated again with electron in the TEM.

3. Results

3. 1 Microstructure before ion implantation

Fig. 1 shows an electron micrograph and electron diffraction patterns after ion thinning. The dark curved lines in the figure are bend contour. The specimen was identified as

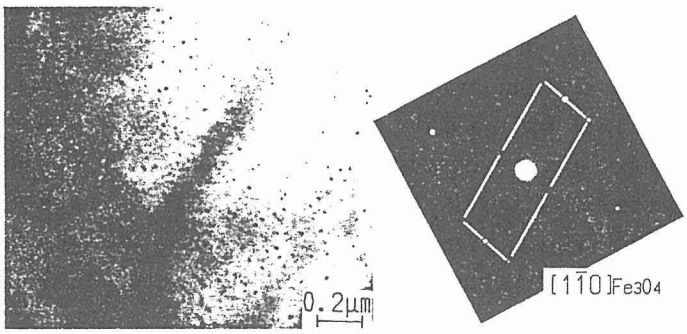

Fig. 1 Electron micrograph of magnetite after Ar ion thinning.
(K. Ishii et al)

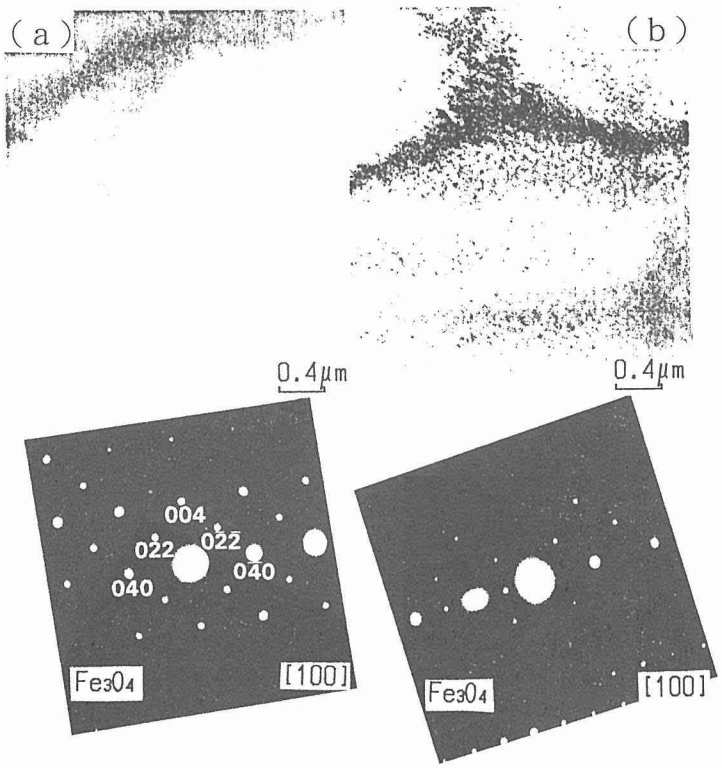

Fig. 2 Electron micrograph of magnetite after Ar ion thinning. (a) Plain structure and (b) heavy defected structure.
(K. Ishii et al)

magnetite from SAD pattern and its optic axis was [100]. There are two typical microstructures of magnetite shown in Fig. 2. Fig. 2 (b) depicts the defect structure introduced by Ar damage during ion thinning and (a) plain structure. The structure of (b) is caused by collision with Ar ions. The SAD pattern in Fig. 2 (b) was taken in the defected area and slightly distorts from ordinary pattern (Fig. 2 (b)) due to heavy defect concentration.

3. 2 Microstructure after hydrogen implantation

In Fig. 3 the region of defect structure, which is shown in Fig. 2 before implantation, is shown after implantation. In the SAD pattern of this region, magnetite and wustite patterns can be seen. It is clear that the formation of wustite is due to hydrogen implantation. The left figure is bright field image and the right figure is dark field image. The orientation relationship between magnetite and wustite was determined in Fig. 4, which is a micrograph of the regions where both magnetite and wustite exist. The optic axes of magnetite and wustite are [110] and [110] and are parallel. This typical orientation relationship is illustrated in Fig. 5 for wustite and magnetite. A (110) plane in magnetite is parallel to the (110) plane in wustite.

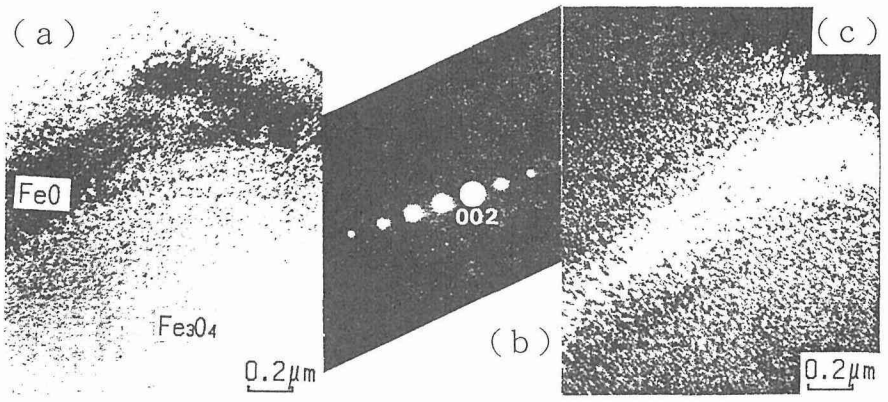

Fig. 3 Electron micrograph of magnetite after H_2 implantation.
(a) Bright field image, (b) SAD pattern and (c) dark field image.
(K. Ishii et al)

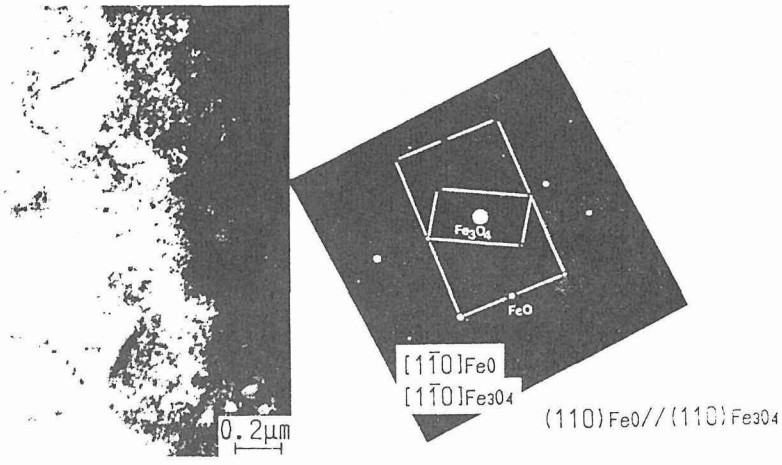

Fig. 4 Electron micrograph of magnetite after H_2 implantation and SAD pattern showing crystallographic relationship between magnetite matrix and precipitated wustite (can not appear in the picture).
(K. Ishii et al)

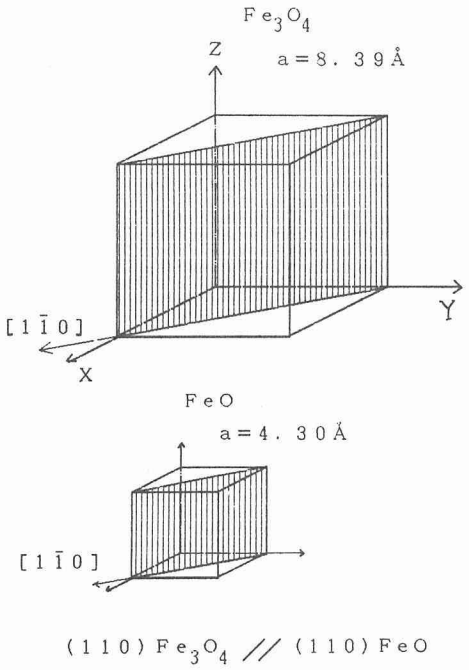

Fig. 5 Schematic diagram showing crystallographic direction of magnetite and wustite after H_2 implantation. (K. Ishii et al)

3.3 Effect of electron irradiation

The effect of irradiation on transfomation of the specimens which were irradiated with electron beam after hydrogen implantation was investigated.

Fig. 6 (a) and (b) are microstructures irradiated by electrons for 2 hours and 4 hours,

Fig. 6 Electron micrographs irradiated by electron beam in TEM after H2 implantation for (a) 2 hours and (b) 4 hours.
(K. Ishii et al)

respectively. After 2 hours irradiation, the evident structural changes due to irradiation were not observed, but a growth of blisters with increasing of irradiation time was observed. Furthermore, the formation of wustite was confirmed by SAD after 4 hours irradiation at the region where only magnetite existed after 2 hours. This fact suggests that electron beams induces the transformation from magnetite to wustite. Fig. 7 is micrograph of the region where both magnetite and wustite exist. Electron diffraction pattern is taken from the center of image. The diffraction pattern is belonging to both the optic axes [110] of magnetite and of wustite. The (001) plane of magnetite is parallel to the (001) plane of wustite. This relation ship is illustrated in Fig. 8, and it is the same as that in the case of wustite formation immediately after hydrogen implantation.

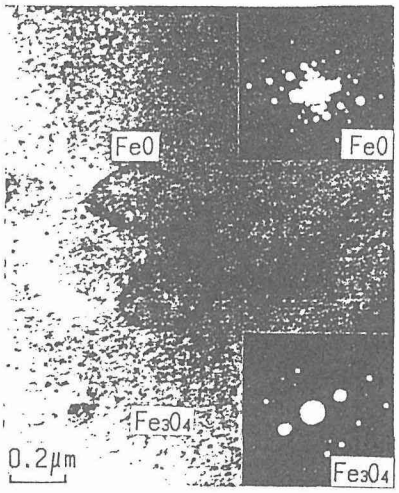

Fig. 7 Electron micrographs irradiated by electron beam in TEM after H2 implantation for 4 hours. Two kinds of SAD patterns were observed, magnetite and wustite.
(K. Ishii et al)

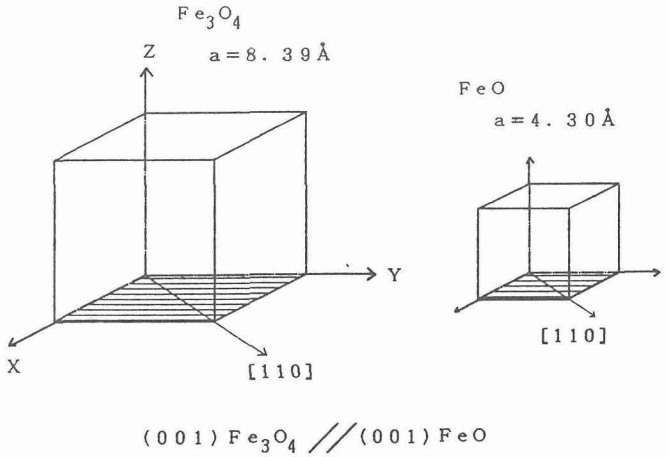

Fig. 8 Schematic diagram showing crystallographic direction of magnetite and wustite after electron beam irradiation.
(K. Ishii et al)

3.4 Change of Lattice constants

Lattice constants of magnetite, which are shown in Table 1, were calculated from interplanar spacing of electron diffraction after ion thinning, hydrogen implantation and electron irradiation. Comparing the value (inverse spinel structure a=8.403A) from ASTM data table, the lattice constant was smaller after ion thinning. After hydrogen implantation, it was as large as the value from ASTM, and then it was enlarged by electron irradiation.

Table 1 Lattice constants of magnetite specimen.

	lattice const.(A)
after Ar thinning	8.35(±0.02)
after H_2 implant.	8.40
after electron irrd.	8.42

4. Discussion

Before implantation, iron and oxygen atoms in magnetite lattice were knocked out by Ar ions during ion milling, so that they changed into interstitial and concentrated partially. The crystal structure of magnetite is inverse spinel structure as shown in Fig. 9 and oxygen atoms occupy the site of face centered cubic lattice. Because oxygen ion is larger than iron ion, it

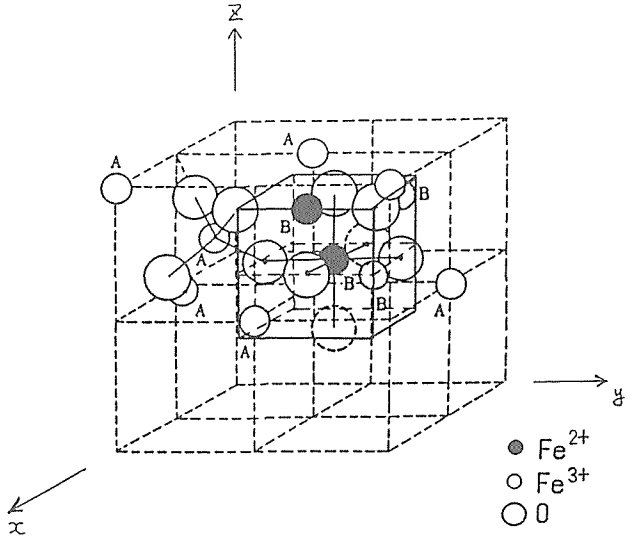

Fig. 9 Schematic diagram of inverse spinel structure.
(K. Ishii et al)

is considered that iron atoms become chiefly interstitial atom. The regions having interstitial atoms, are richer in Fe than other regions. However wustite was not observed actually after ion milling. It suggests that not only interstitial irons but other cations also

are indispensable to form wustite. Magnetite is expressed by $Fe^{3+}(Fe^{2+}Fe^{3+})O^{2-}{}_4$ in which Fe^{3+} is more than Fe^{2+}, the ratio between Fe^{2+} and Fe^{3+} is 1 : 2, so interstitial ions are expected to be mostly Fe^{3+}. Considering that, the reaction of wustite formation is written as

$$Fe^{3+}(Fe^{2+}Fe^{3+})O^{2-}{}_4+Fei^{3+}+3e^-=4\ Fe^{2+}O^{2-} \tag{3}$$

where, $Fe^{2+}O^{2-}$ is wustite and Fei^{3+} is interstitial ion. It indicates that electrons are needed to form wustite, and are not supplied by ion spattering. In ion implantation, hydrogen ions interact to Fe or O ions and lose the energy by ionization and/or excitation by capture or loss of electron. In the last time, hydrogen ions are trapped as coordination and Fe^{3+} ions turn into Fe^{2+} capturing electron. The reaction caused by implantation is

$$Fe^{3+}(Fe^{2+}Fe^{3+})O^{2-}{}_4+Fe^{3+}+3H=4\ Fe^{2+}O^{2-}+3H^+ \tag{4}$$

where H is implanted hydrogen and H^+ is trapped hydrogen. Hydrogen is implanted as H_2 and H^+, so approximately half of implanted hydrogen is trapped as H^+ without providing electron for Fe^{3+}.

At the wustite formation by electron irradiation, the threshold energy to knock on iron atom is calculated to 328keV using the displacement energy of iron atom, 17-22eV[12]. It is considered that radiation damage is hardly obtained because the electron energy is 200keV in this study. Implanted hydrogen atoms are not uniform in distribution and blisters are formed at the part where the concentration of hydrogen is high. In this part, trapped hydrogen and radiated electron interact with magnetite, so wustite formation occur near the blisters. The reaction is written as

$$Fe^{3+}(Fe^{2+}Fe^{3+})O^{2-}{}_4+2H^++2e^-=3Fe^{2+}O^{2-}+H_2O \tag{5}$$

Hydrogen ions are trapped at the interstitial sites of magnetite by implantation and get electron from electron beam. Oxygen in magnetite combines with the hydrogen. As a result, oxygen is removed from magnetite and wustite is formed.

Relation between the mechanisms of transformation mentioned above and the changes of lattice constant of magnetite shown in Table 1 is considered as follows. After ion thinning, the lattice constant is smaller than an ordinary value. It suggests that atoms of magnetite lattice are knocked by Ar ions during ion thinning. Fe ions left behind are Fe^{2+} more than Fe^{3+} and Fe^{2+} changes to Fe^{3+} to maintain the electron neutrality. Ionic radius of Fe^{2+} is 0.83Å and of Fe^{3+} is 0.67Å. Therefore, lattice constant becomes small. After hydrogen implantation lattice constant recovered as large as an ordinary value. The reason is because implanted hydrogen ions enter into magnetite and Fe^{3+} ions change to Fe^{2+} to maintain the electron neutrality. Furthermore lattice constant is enlarged during electron radiation because of lattice expansion due to wustite precipitation.

Fig. 9 illustrates a crystal structure of magnetite, in which it is considered that NaCl type wustite lattice is formed based on oxygen atoms in magnetite lattice drawn by a solid line.

The orientation relationship after implantation mentioned above is the same as that induced by electron irradiation, though expressions of the orientation are different. In the

case of wustite formation because of electron irradiation, (001) plane of wustite is formed from (001) plane of magnetite, the orientation relationship is depicted to make clear of atomic changes in Fig. 10, which illustrate the cross section of magnetite lattice parallel to (001) plane, where dushed lines express new wustite phase and arrows indicate the shift direction of atoms. In this case oxygen ions do not move and iron ions are moved to wustite sites from lower planes. The sum of the moving distance of atoms in a wustite unit is 5.47 Å and the spacing of these ions are expanded about 8% into wustite lattice.

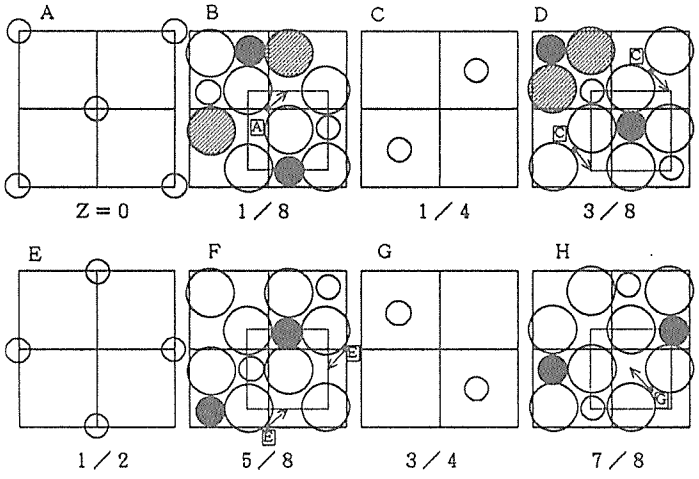

Fig. 10 Schematic diagram of crystallographic relationship between magnetite and wustite after electron beam irradiation.
(K. Ishii et al)

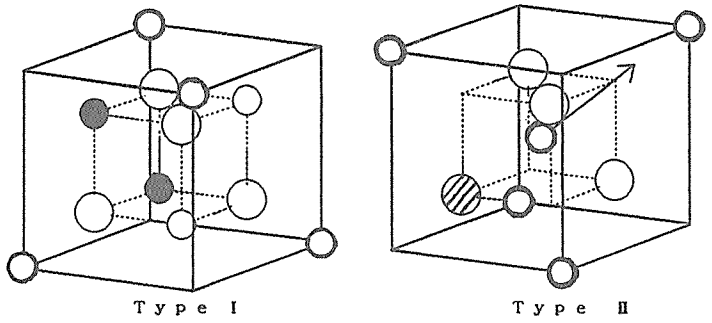

Fig. 11 Schematic diagram of two types of magnetite lattice.
(K. Ishii et al)

Fig. 11 illustrates two types of magnetite lattice. The largest spacing volume is the center of cubic (octahedral site) and vacancies of oxygen sites of inner cubic (tetrahedral site), so it is considered that implanted hydrogen can be trapped in these sites. The arrow illustrates the shift direction shown in Fig. 10 and oxygen which disturb in moving of iron is hatched. Implanted hydrogen is considered to be coordinated to surround this oxygen.

5. Conclusion

Hydrogen ion implantation was carried out for magnetite to study the crystallographic mechanism of H_2 reduction. Before hydrogen implantation there are two typical structure of magnetite, one is a defect structure caused by Ar spattering and the other has few defects. In the place where the defects introduced by Ar were concentrated, wustite was formed in magnetite as soon as hydrogen was implanted. In this case, the orientation relationship between wustite and magnetite was (110)FeO//(110)Fe_3O_4. The wustite was also formed by cooperation of implanted hydrogen and irradiated electron during TEM observation and the orientation relationship was determined as follows; (001)FeO//(001)Fe_3O_4 and [110] FeO// [110] Fe_3O_4. Two relationships are the same.

References

1) A. V. Bradshaw and A. G. Matyas: Metall. Trans., 7B (1976), 81
2) M. Moukassi, P. Steinmetz, B. Dupre and C. Cleitzer: Metall. Trans., 14B (1983), 125
3) D. H. St. John, S. P. Matthew and P. C. Hayes: Metall. Trans., 15B (1984), 709
4) B. Deo, S. Chatterjee and R. K. Dube: Steel Research, 59 (1988), 532
5) P. R. Swann and N. J. Tighe: Metall. Trans., 8B (1977), 479
6) S. P. Matthew and P. C. Hayes: Metall. Trans., 21B (1990), 141
7) M. Rau, D. Rieck and J. W. Evans: Metall. Trans., 18B (987), 257
8) C. J. Mchargue: Nucl. Instrum. Methods, B19/20 (1987), 797
9) C. J. Mchargue: Nucl. Instrum. Methods, B16 (1986), 212
10) C. J. Mchargue: Nucl. Instrum. Methods, B19/20 (1987), 809
11) A. P. Mouritz: Nucl. Instrum. Methods, B19/20 (1987), 805
12) P. Jung: Atomic Collisions in Solids., Plenum Press, New York, (1975), 87